

Electrochemical Detection of Single Molecules

ALLEN J. BARD* AND FU-REN F. FAN

Department of Chemistry and Biochemistry, The University of Texas at Austin, Austin, Texas 78712

Received June 7, 1996

A study of the electrochemical behavior of single molecules requires measurement of the small current that flows as a result of electron-transfer reactions at an ultramicroelectrode. Such studies would be of use in determining half-reaction potentials, free energies, and reaction kinetics with tiny samples. They would also represent the ultimate sensitivity for electroanalytical detection. Moreover, as with other single-molecule techniques, there is the expectation that investigations of single molecules and molecular events will allow one to uncover phenomena and properties that are not apparent when one observes processes involving a large number of molecules, as is typical in conventional electrochemical experiments. The molecules usually investigated in electrochemical experiments are either freely diffusing in solution or adsorbed or attached to an electrode surface or membrane. Single-molecule electrochemical detection (SMED) of both types are of interest.

We have been investigating two approaches to SMED. The first involves trapping an electroactive molecule in solution between a small ultramicroelectrode tip and a conductive substrate in a scanning electrochemical microscope (SECM).¹ In this arrangement, the tip current represents repeated collisions and electron transfers of the molecule with the tip. An alternative approach is to use electrogenerated chemiluminescence (ECL) in which the product of the electron transfer of the electroactive molecule, e.g., its oxidized form, reacts to form an excited state that emits a photon.^{2,3}

Single-Molecule Electrochemistry

Scanning Electrochemical Microscopy. Trapping of a molecule in solution and detection of the electrolysis current are carried out in an SECM.⁴ This instrument is based on observing the electrolysis of an electroactive species, A, at a very small (nm– μm) electrode (an ultramicroelectrode or SECM tip) to form a product, B, as shown in the following reduction reaction:



The current that flows represents the flux of A to the electrode as it diffuses to the tip. In the SECM, the tip potential is controlled and the current is measured with standard electrochemical instrumentation while the movement of the tip is carried out with piezoelec-

tric elements as in other scanning probe techniques (Figure 1). SECM studies are based on moving the tip very close to a surface (i.e., to within about the tip diameter) and observing how the tip current (i_T) changes compared to that when the tip is far from the surface ($i_{T,\infty}$). The surface can affect the tip current in two different ways. When the tip is close, diffusion is blocked; this causes a decrease in the current. If, however, the product of the tip reaction B can be oxidized back to A at the surface, then an additional flux of A to the tip occurs (termed positive feedback), and the tip current is increased compared to $i_{T,\infty}$. Thus, a plot of i_T vs d (the distance between the tip and the surface) can provide information about the nature of the surface. If the tip is a conductive disk in an insulating plane, the tip radius a can be found with the equation

$$i_{T,\infty} = 4nFDCa \quad (2)$$

where D is the diffusion coefficient of A, C is its concentration, and F is Faraday's constant. The approach curve can also be used to obtain some idea about the tip geometry.^{1,5} This is particularly useful for tips of submicrometer size, which are difficult to image by electron microscopy. Typical approach curves for disk-shaped tips that are found experimentally and are derived by digital simulation of the mass-transfer conditions in the SECM⁶ are shown in Figure 2 (curves 1 and 2).

The single-molecule trapping experiments require a tip with a diameter on the order of 10–20 nm and the particular geometry that results from the procedure used in tip preparation. The tip is made by electrochemical sharpening of a Pt–Ir (80:20) wire (0.250-mm diameter). The tip is completely insulated by passing it through molten Apiezon wax or polyethylene. A hole is then produced at the very end by mounting the tip in the SECM apparatus and moving it toward the substrate until a current on the order of a picoamperes flows.⁷ This produces a tip that shows the approach curve in Figure 2 (curve 3), suggesting a geometry very different from that of the disk electrode in a plane, which produces curves 1 and 2. A reasonable fit to this curve is obtained by simulating a tip that is slightly recessed within the insulating film of wax to form a small pocket, as shown sche-

(1) Fan, F.-R.; Bard, A. J. *Science* **1995**, *267*, 871.

(2) Bard, A. J.; Faulkner, L. R. In *Electroanalytical Chemistry*; Bard, A. J., Ed.; Marcel Dekker: New York, 1977; Vol. 10, p 1.

(3) Collinson, M. M.; Wightman, R. M. *Science* **1995**, *268*, 1883.

(4) Bard, A. J.; Fan, F.-R.; Mirkin, M. V. In *Electroanalytical Chemistry*; Bard, A. J., Ed.; Marcel Dekker: New York, 1994; Vol. 18, pp 243–373.

(5) Mirkin, M.; Fan, F.-R.; Bard, A. J. *J. Electroanal. Chem. Interfacial Electrochem.* **1992**, *328*, 47.

(6) Kwak, J.; Bard, A. J. *Anal. Chem.* **1989**, *61*, 1221.

(7) Nagahara, L. A.; Thundat, T.; Lindsay, S. M. *Rev. Sci. Instrum.* **1989**, *60*, 3128.

Allen J. Bard holds the Hackerman-Welch Regents' Chair in Chemistry at the University of Texas at Austin. His principal research interests are in the application of electrochemical techniques to the study of chemical problems.

Fu-Ren F. Fan received his B.S. from National Taiwan University, his M.S. from Kent State University, and his Ph.D. from the University of Illinois in the area of photovoltaic and photoelectrochemical effects of phthalocyanines. He is currently working as a Research Scientist Associate in the area of electroanalytical chemistry in Dr. Bard's Laboratory of Electrochemistry at the University of Texas at Austin.

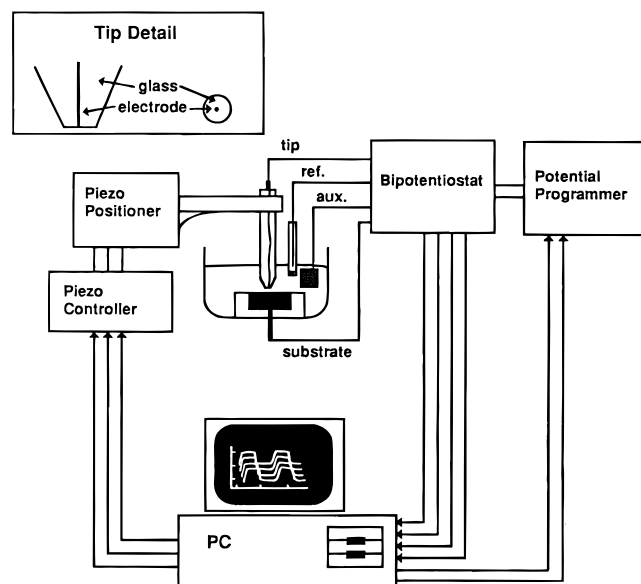


Figure 1. SECM apparatus. Reprinted with permission from Bard, A. J.; Denuault, G.; Lee, C.; Mandler, D.; Wipf, D. O. *Acc. Chem. Res.* **1990**, *23*, 357. Copyright 1990 American Chemical Society.

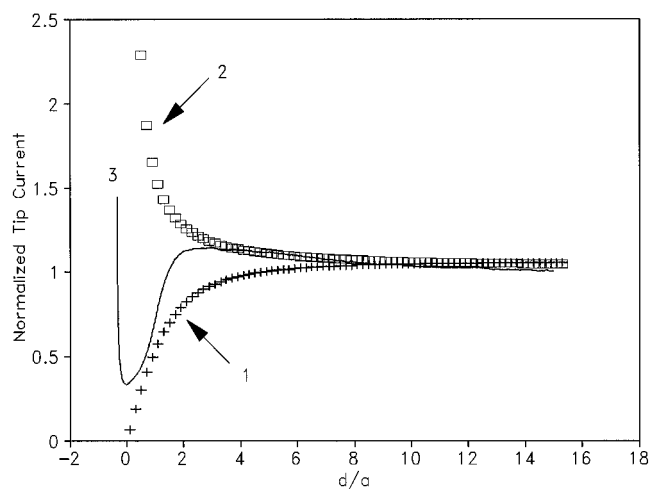


Figure 2. SECM approach curves: (1) disk-shaped tip, insulating substrate, (2) disk-shaped tip, conductive substrate, (3) recessed tip, conductive substrate.

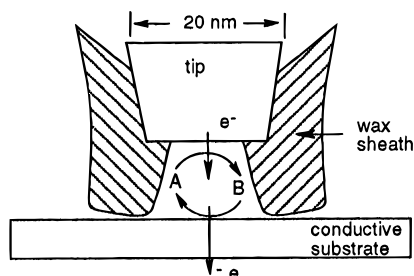


Figure 3. Single-molecule detection with the SECM. Molecule A trapped between the tip and surface. Reprinted with permission from ref 8. Copyright 1996 American Chemical Society.

matically in Figure 3.⁸ It is our experience that the production of submicrometer tips by drawing metal wires in glass often produces tips in which the conductor is slightly recessed within the insulator. Most of these show approach curves with a conductive sub-

(8) Fan, F.-R.; Kwak, J.; Bard, A. J. *J. Am. Chem. Soc.* **1996**, *118*, 9669.

(9) Smith, C. P.; White, H. S. *Anal. Chem.* **1993**, *65*, 3343.

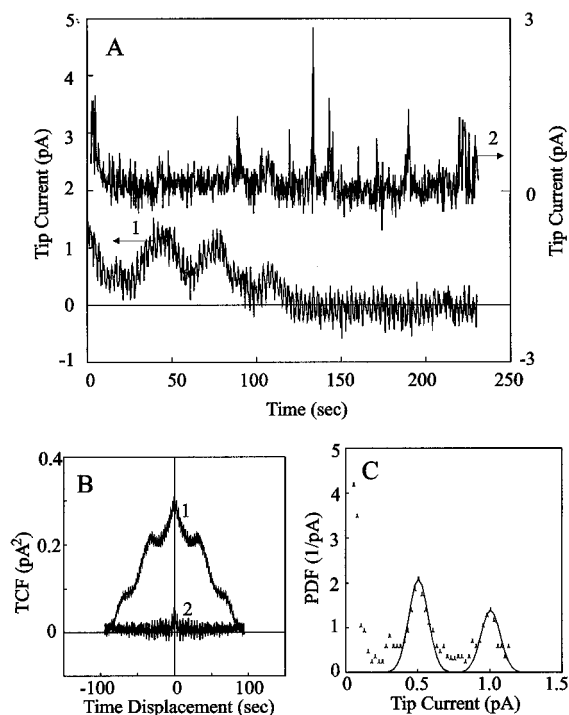


Figure 4. (A) Curve 1: Tip current with time for a solution of 2 mM CpFeCpTMA⁺ and 2.0 M NaNO₃ with a Pt-Ir tip at 0.55 V vs SCE and an ITO substrate at -0.3 V; $d \approx 10$ nm. Curve 2: Time series of the tip current for d within the tunneling range in a solution containing only 2.0 M NaNO₃; tip radius ~ 7 nm. Data sampling rate 0.4 s per point. (B) Corresponding time correlation functions. (C) Probability density function of time series 1 in (A). Reprinted with permission from ref 8. Copyright 1996 American Chemical Society.

strate in which the current remains almost constant or shows a small amount of positive feedback and then limits as the insulator contacts the substrate.

Single-Molecule Detection Experiment. Current instrumentation does not allow measurement of the charge or current from single-electron-transfer events at an electrode. To detect a single molecule electrochemically, one must provide some amplification process. In the SECM experiment, illustrated schematically in Figure 3, this amplification is provided by the positive feedback process, i.e., the repeated conversion of A to B at the tip and B to A at the substrate as the molecule, in the oxidized or reduced state, shuttles back and forth between the tip and substrate. The transport between the two electrodes is by diffusion, so that the transit time (τ) between the tip and surface separated by a distance d is about $d^2/2D$. If $d = 10$ nm and $D = 10^{-5}$ cm²/s, then $\tau = 5 \times 10^{-8}$ s or the molecule cycles 10^7 times per second. If each cycle results in the exchange of one electron (1.6×10^{-19} C), then an average current of about 1.6 pA will flow. Thus, positive feedback provides a 10-million-fold amplification that results in a readily measurable current. It is necessary, however, to trap the molecule within the small pocket formed by the surrounding insulator in the gap between the tip and substrate for a sufficient time to make the measurement, which is governed by the time constant of the picoammeter. Figure 4A shows an experiment with a water soluble ferrocene derivative as the species oxidized at the tip to produce the ferrocenium form that is then reduced at the indium tin oxide (ITO) substrate.¹ In this experiment, the tip

(radius ~ 10 nm) was brought to a position where the approach curve (like curve 3 in Figure 2) was near its minimum value, estimated as about 10 nm. At the concentration of electroactive species employed, the resultant volume under the tip would contain, on the average, one molecule of ferrocene. When the current at the tip is recorded with time, one finds fluctuations of the current (on top of the noise signal on the order of 0.2 pA), which were interpreted to indicate the presence of zero, one, or two molecules. This finding is clarified by examining the data by autocorrelation and probability density function (PDF) analyses (Figure 4B,C).⁸ The time correlation function (TCF) analysis indicated multiple fluctuation processes with the frequencies of fluctuation on the order of a few tenths of a hertz. The PDF contains several bell-shaped peaks. The most probable tip currents at the given cell parameters and concentrations are spaced $0.5 (\pm 0.1)$ pA apart. These fluctuation amplitudes of the tip current–time series correspond quite well with the contribution to the current expected for a single molecule in a thin-layer cell of that geometry. Control experiments with the tip at longer and closer distances to the ITO and with two different species that oxidize at two different potentials are consistent with this interpretation.

A quantitative interpretation of the current–time behavior is not possible without a better understanding of the tip shape and drift. The approach curve in Figure 2 (curve 3) has been reproduced by a finite difference treatment of an idealized disk-shaped conductor that is slightly recessed within a cylindrical compartment of the wax insulator.⁸ The decrease in the current at close approach is largely due to diffusion to the tip being hindered by the substrate and by a decrease in the area of the conductor as the wax is squeezed against the ITO. The increase in current shown in curve 1 of Figure 4A signals the entrance of an electroactive molecule into the tip–ITO gap. The slow rise and fall in the current signal is attributed to a slow continuous drift of the tip toward and away from the substrate, probably caused by thermal fluctuations and mechanical relaxation of the piezoelements, which would superimpose a long-term rise and fall in the tip current.

Because of the extreme sensitivity of the experiment to temperature changes and vibration, it is not possible to change conditions with the tip near the surface, e.g., by changing the solution composition or replacing the substrate, without damaging the tip. However, by proper choice of solution or substrate, one can perform experiments that show the effects of such changes on the tip current–time behavior. For example, one can choose two different electroactive molecules that are oxidized at different potentials (e.g., a ferrocene and $\text{Os}(\text{bpy})_3^{2+}$) and so control the effective concentration of electroactive species by controlling the potential where one, both, or neither is oxidized.¹ One can also use an n-type semiconductor, e.g., TiO_2 , as a substrate.⁸ By controlling the potential of the semiconductor, it can be made to behave as either a conductor (in the accumulation region) or an insulator (in the depletion region). Thus, one can show with the same solution and tip that positive feedback and the fluctuating current response occur when the TiO_2 is conductive, but no response is observed when it is insulating (Figure 5).⁸

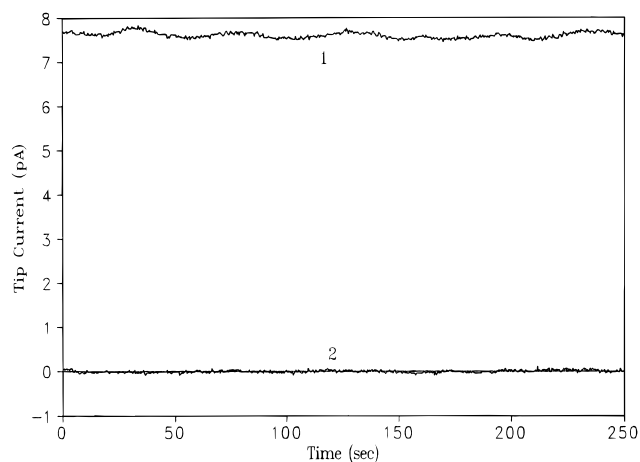


Figure 5. Tip current for a solution of 2 mM CpFeCpTMA^+ and 1.0 M NaNO_3 with a Pt–Ir tip at 0.6 V vs SCE and titanium dioxide substrate at (1) -0.7 and (2) 0.0 V vs SCE. $d \approx 13$ nm. Reprinted with permission from ref. 8. Copyright 1996 American Chemical Society.

Projected Experiments. Many additional experiments remain to be done in SMED. For example, the current fluctuations mapped as the spectral density function should be related to the probability of the number of molecules in the tip–substrate gap as a function of solution composition. At a solution concentration of 2 mM for a solution volume of 10^{-18} cm^3 , for example, the average occupancy is one molecule. However, the actual occupancy, because of fluctuations, is governed by the Poisson distribution,

$$f_a(n) = a^n \exp(-a)/n! \quad (3)$$

where $f_a(n)$ is the probability of n molecules occupying the solution volume when the average occupancy is a . Thus, for $a = 1$, $f_a(0) = 0.368$, $f_a(1) = 0.368$, and $f_a(2) = 0.184$. The distribution shown in Figure 4 approaches this, favoring slightly less than an average of one molecule per gap volume. All of the experiments described above were carried out with a high concentration of supporting electrolyte, so that electric field effects on the movement of the electroactive molecules were negligible. However, at low electrolyte concentrations, electrical migration effects, in addition to diffusion, should be important; i.e., when the electroactive molecules make a significant contribution to the ionic strength, their movement to maintain electroneutrality (and double-layer charge equilibrium) contributes to their flux and hence to the current.

Recently the validity of the assumption of electro-neutrality or diffusion-controlled transport on electrodes of dimensions of less than ca. $0.1 \mu\text{m}$ has been raised.⁹ While single-molecule detection experiments have not been carried out, we have performed several sets of SECM experiments to address this problem. The first involves oxidative voltammetric measurements on a positively-charged species [(trimethylammonio)methyl]ferrocene (CpFeCpTMA^+) at various gap separations d . The second experiment compared the limiting tip current for the oxidation of a positively-charged species (CpFeCpTMA^+), a singly negatively-charged species (CpFeCpCOO^-), and a doubly negatively-charged species ($\text{Fe}(\text{CpCOO}^-)_2$). This experiment was performed by biasing the tip potential (E_T) at a constant value, 0.6 V vs a platinum quasi-

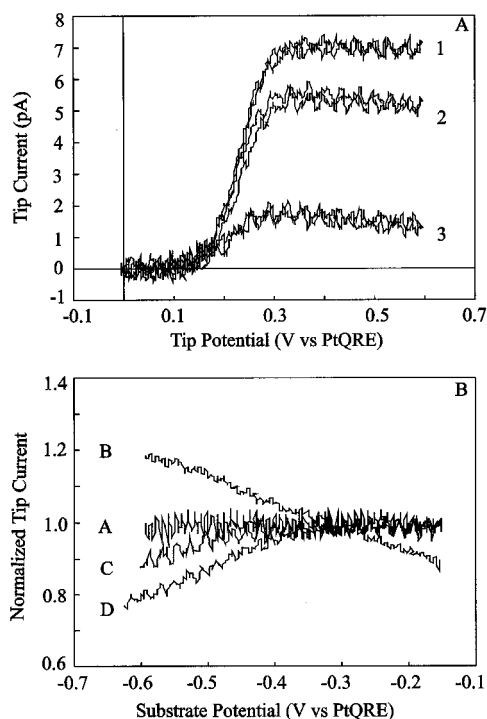


Figure 6. (A) Cyclic voltammograms of 2 mM CpFeCpTMA⁺ in an aqueous solution containing no supporting electrolyte at a Pt tip ($a \approx 18$ nm) at three different gap separations. Curve 1: Tip held far away from the surface. Curve 2: Tip at a distance within the range where the tip current started to decrease with decreasing distance. Curve 3: Tip closer to the surface as compared with 2. Tip potential scan rate 5 mV/s for all cases. (B) Tip limiting current at $E_T = 0.6$ V vs PtQRE as a function of the substrate potential for different charged species. Curve A: 2 mM CpFeCpCOO⁻ in 1.0 M NaNO₃. Curve B: 2 mM CpFeCpTMA⁺, no supporting electrolyte. Curve C: 2 mM CpFeCpCOO⁻, no supporting electrolyte. Curve D: 2 mM Fe(CpCOO⁻)₂, no supporting electrolyte. All limiting tip currents normalized with respect to the limiting tip current of curve A at $E_S = -0.3$ V vs PtQRE. Substrate potential scan rate 5 mV/s.

reference electrode (PtQRE), to obtain a limiting anodic tip current. The tip current was then monitored while the substrate potential (E_S) was scanned.

As shown in Figure 6A, when the tip ($a \approx 18$ nm) was far from the ITO substrate, a steady-state plateau-shaped cyclic voltammogram was obtained for the oxidation of CpFeCpTMA⁺ in an aqueous solution containing no supporting electrolyte. When the tip was brought to a distance within the range where the tip current started to decrease significantly with decreasing d , a steady-state, somewhat peak-shaped voltammogram was obtained (curve 2). The dramatic decrease in the tip current with decreasing distance, as discussed previously, is mainly due to diffusion to the tip being hindered by the substrate and by the decrease in the tip area as the tip is pushed against the ITO substrate. The peaking became more evident as the tip was brought even closer to the surface (curve 3). No evident peaking under such conditions was observed in the presence of 1.0 M NaNO₃. The results of the second experiment are shown in Figure 6B. When the tip was far away from the ITO surface, the tip current, as expected, was essentially independent of E_S in the potential range studied. However, at small d , a significant increase in the limiting tip current with CpFeCpTMA⁺ (or decrease with CpFeCpCOO⁻) was observed when the substrate

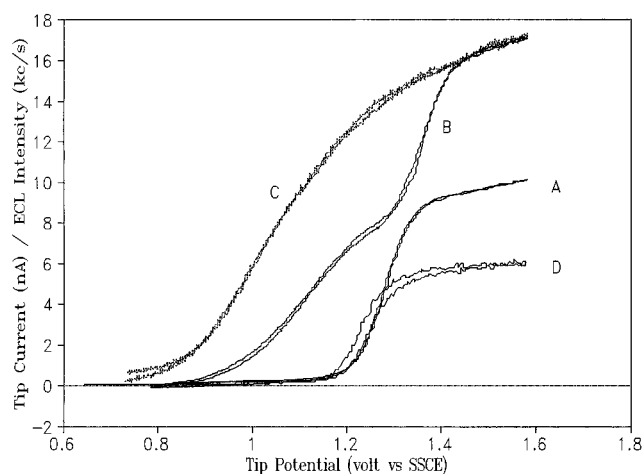


Figure 7. (A) Cyclic voltammogram of 1 mM Ru(bpy)₃²⁺ in an acetonitrile solution containing 0.2 M TBABF₄ (supporting electrolyte) at a Pt microdisk electrode ($a = 12.5$ μm). (B) After addition of 0.5 mM TPrA to the solution used in (A). (C) Cyclic voltammogram of 1 mM TPrA in an acetonitrile solution containing 0.2 M TBABF₄. (D) Corresponding ECL intensity vs potential curve for an acetonitrile solution containing 1 mM Ru(bpy)₃²⁺, 3.5 mM TPrA, and 0.2 M TBABF₄. Tip potential scan rate 5 mV/s for all cases.

potential was scanned toward more negative potentials. The higher the charge of the species, the more significant was the effect (compare C with D). Both sets of experimental results show that the limiting tip currents show significant potential dependence (ca. 20% increase or decrease) only at small d and very low supporting electrolyte concentration. Although they can be qualitatively understood on the basis of the double-layer effects,^{10,11} a quantitative interpretation of these voltammetric curves requires more rigorous simulation.⁹

It should also be possible to measure single-molecule homogeneous kinetics in an electrochemical experiment, e.g., by introducing a higher concentration of an electroinactive species, Z, that reacts with the tip-generated species to produce the starting molecule, i.e.,



Thus, when B is generated at the tip, in addition to the feedback provided by B diffusing to the substrate to form A, which diffuses back to the tip, A can be regenerated by reaction with Z. This type of reaction, called a catalytic or EC' reaction mechanism,¹¹ should lead to an increased average current. The extent of the increase should be useful in estimating the rate constant of the reaction in eq 4. This reaction scheme is also of importance in the ECL experiments described below.

It is of interest to consider if single-electron-transfer events might ultimately be detectable at electrodes or interfaces. The problem is to detect the difference a single electron makes in the measured signal above any noise. Such single-electron events are seen at very small metal structures (quantum dots) at low temperatures in so-called "Coulomb blockade" experiments.¹² For example, consider the capacitance of an

(10) Delahay, P. *Double Layer and Electrode Kinetics*; Interscience Publishers: New York, 1965; pp 153–167.

(11) Bard, A. J.; Faulkner, L. R. *Electrochemical Methods*; Wiley: New York, 1980.

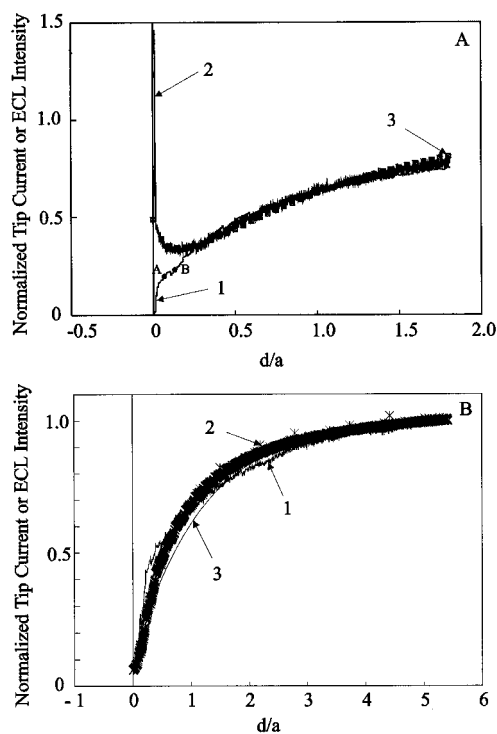


Figure 8. (A) Distance dependence of the ECL intensity (curve 1, solid line) and tip current (curve 2, dotted line) over a conducting substrate (ITO) in an acetonitrile solution containing 1 mM Ru(bpy)₃²⁺, 20 mM TPrA, and 0.2 M TBABF₄. Tip (*a* = 12.5 μm) and substrate biased at 2.1 and -0.30 V vs SSCE, respectively. Curve 3 (squares): simulated tip current approach curve based on 95% contribution from the totally-irreversible oxidation of TPrA and 5% contribution from the reversible oxidation of Ru(bpy)₃²⁺. (B) Distance dependence of the ECL intensity (curve 1, dotted line) and tip current (curve 2, asterisks) over an insulating substrate (quartz) in an acetonitrile solution containing 1 mM Ru(bpy)₃²⁺, 20 mM TPrA, and 0.2 M TBABF₄. Tip (*a* = 12.5 μm) potential continuously pulsed (pulse width *t* = 10 ms) between 2.1 and 0.1 V vs SSCE to generate ECL. Both the ECL intensity and tip current sampled at 0.05*t* prior to the end of each anodic pulse. Curve 3 (solid line): simulated SECM approach curve for the insulating substrate.

electrode with an area of 1000 nm². If its differential capacitance is the same as that of a typical larger electrode, ~10 μF/cm², then its capacitance would be 10⁻¹⁶ F. The addition of a charge corresponding to a single electron (1.6 × 10⁻¹⁹ C) would produce a voltage change of 1.6 mV. If a suitable high input impedance device is available, such a charge step would be measurable. An alternative approach would involve some inherent amplification process, analogous to the cascade in electrons in a photomultiplier or channel plate triggered by a single photon or energetic particle. An example of this in an interfacial scheme would be a single event at a membrane channel that causes a large flux of ions through the channel and a measurable current flow.

Electrogenerated Chemiluminescence

Basic Principles. Since single-photon events can be monitored, reactions of electrogenerated species that produce light (ECL) can also be used to track

(12) *Single Charge Tunneling (Coulomb Blockade Phenomena in Nanostructures)*; Grabert, H., Devoret, M. H., Eds.; NATO ASI Series B; Plenum: New York, 1992; Vol. 294.

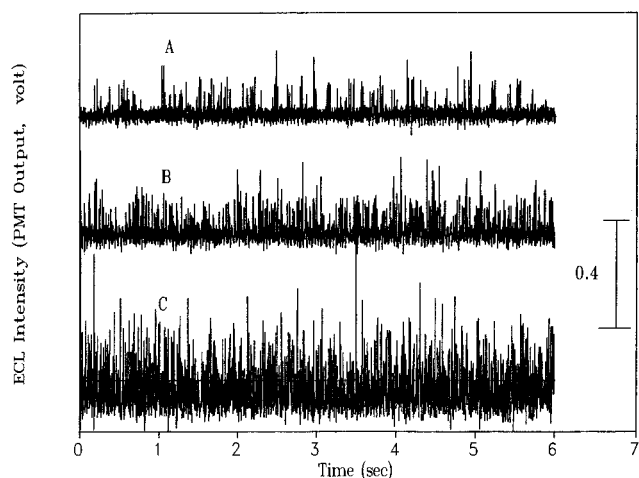


Figure 9. Histograms of the ECL intensity sampled at 1 kHz for three different gap separations between the tip and ITO substrate. Curves A, B, and C for *z* positions marked A and B in Figure 8A and for the tip far away from the substrate, respectively. Tip (*a* = 12.5 μm) and substrate biased at 2.1 and -0.3 V vs SSCE, respectively, during ECL generation in an acetonitrile solution containing 1 mM Ru(bpy)₃²⁺, 20 mM TPrA, and 0.2 M TBABF₄.

individual events near an electrode. The basic principles of ECL have been extensively reviewed.^{2,13,14} As shown in eq 5, when a strong electron donor, A⁻ reacts



with a strong electron acceptor, D⁺, the electron-transfer reaction can produce an excited state, ¹A*. This species can emit a photon. The same principles apply when A⁻ and D⁺ are, respectively, the reduced and oxidized forms of the same starting material. ECL is usually generated by producing the reactants electrochemically, either at a single electrode by alternately pulsing the electrode to produce A⁻ and D⁺ or at a closely spaced pair of electrodes by a steady-state technique (e.g., the rotating ring-disk electrode,¹⁵ the double-band electrode,¹⁶ or the thin-layer cell¹⁷).

Observation of Individual Chemical Reactions in Solution. By using an ultramicroelectrode (UME) and observing events with high temporal resolution, Collinson and Wightman³ have recently been able to observe discrete chemical reaction events occurring in solution by single-photon detection of the product of the ECL reaction. The reactants were generated from 9,10-diphenylanthracene (DPA) in acetonitrile with potential pulses applied to the UME to produce DPA⁻ and DPA⁺. When events during a single cathodic pulse following an anodic pulse were viewed with high temporal resolution, ECL emission from individual electron-transfer reaction events was resolved. The stochastic nature of these events followed a Poisson distribution as described by eq 3, in which *a* = λ*t*, *n* is the number of cathodic pulses evaluated, and λ is the

(13) Hercules, D. M. *Acc. Chem. Res.* **1969**, *2*, 301.

(14) Tachikawa, H.; Faulkner, L. R. In *Laboratory Techniques in Electroanalytical Chemistry*; Kissinger, P. T., Heineman, W. R., Eds.; Marcel Dekker: New York, 1984; pp 660-674.

(15) Maloy, J. T.; Prater, K. B.; Bard, A. J. *J. Am. Chem. Soc.* **1971**, *93*, 5959.

(16) Amatore, C.; Fosset, B.; Maness, K. M.; Wightman, R. M. *Anal. Chem.* **1993**, *65*, 2311.

(17) Laser, D.; Bard, A. J. *J. Electrochem. Soc.* **1975**, *122*, 632.

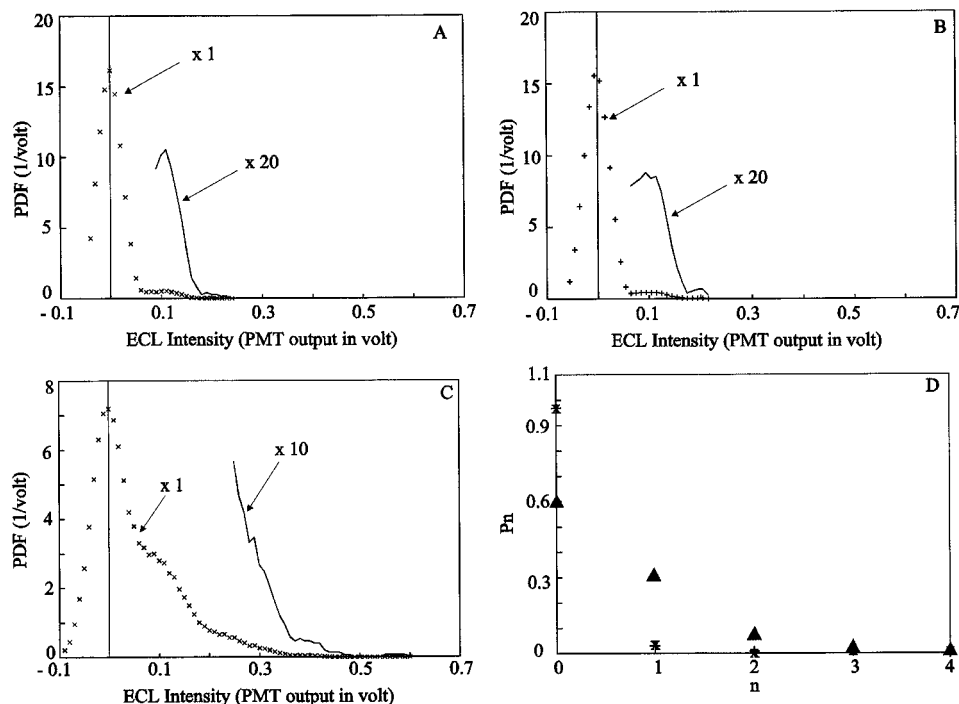


Figure 10. (A–C) Probability density functions of the time series shown in Figure 9. (D) Poisson distributions for PDFs shown in (A) (pluses), (B) (crosses), and (C) (triangles).

mean rate of events. A histogram of the time between individual photons shows an exponential distribution which gives λ . The measured value of λ depended on the concentration of DPA. At concentrations greater than 20 mM, λ was found to be first order in [DPA]. However, a higher order was obtained as the concentration was lowered. This concentration-dependent behavior was attributed to the transition from a diffusion-limiting to a rate-limiting process.³

ECL Probe for SECM. We have recently explored the possibility of utilizing ECL as the probe for SECM on the basis of the luminescent properties of a substrate and the different mechanisms by which the substrate surface can affect the tip current and the ECL intensity. Instead of using the multicycle pulsing technique described above, steady-state ECL was generated at an UME by oxidizing D ($\text{Ru}(\text{bpy})_3^{2+}$, $\text{bpy} = 2,2'$ -bipyridine) in the presence of a coreactant.¹⁸ A coreactant in ECL is a species that produces a reducing agent upon oxidation which can react with the oxidized D ($\text{Ru}(\text{bpy})_3^{3+}$) to produce the excited state. Tri-*n*-propylamine (TPrA) was selected as the coreactant. With this species, the reducing agent is proposed to be the deprotonated oxidized TPrA radical, $\text{Pr}_2\text{NC}^-\text{HEt}$.^{19,20} In an acetonitrile solution containing 0.5 mM TPrA, 1 mM $\text{Ru}(\text{bpy})_3^{2+}$, and 0.2 M TBABF₄ (as the supporting electrolyte), a wave corresponding to the oxidation of TPrA occurs at $E_{1/2} = 1.1$ V vs SSCE (saturated sodium chloride calomel electrode). A second wave occurring at $E_{1/2} = 1.3$ V vs SSCE is associated with the oxidation of $\text{Ru}(\text{bpy})_3^{2+}$ (Figure 7). By scanning the tip to a potential where both TPrA and $\text{Ru}(\text{bpy})_3^{2+}$ are oxidized, fairly strong and steady ECL is observed. The ECL wave coincides with the oxidation wave of $\text{Ru}(\text{bpy})_3^{2+}$, although the ECL

intensity at high [TPrA] tends to decrease with increasing anodic tip bias after reaching a maximum.²¹

Distance Dependence of the Tip Current and ECL Intensity. Figure 8A shows the tip current and ECL intensity approach curves at constant tip bias (2.1 V vs SSCE) over a conductive surface (ITO). The ECL intensity decreases monotonically as the tip approaches the substrate. However, the tip current decreases to a minimum and then increases as the tip comes even closer before showing a very sharp increase because of the onset of electron tunneling between the tip and ITO. With the start of electron tunneling, the ECL intensity drops sharply to zero. The experimental tip current approach curve coincides well with a theoretical curve on the basis of the assumption that the total tip current is a combination of the contribution from the totally irreversible oxidation of TPrA (95%) and the reversible oxidation of $\text{Ru}(\text{bpy})_3^{2+}$ (5%). The current increase associated with the oxidation of $\text{Ru}(\text{bpy})_3^{2+}$ comes from two sources: the regeneration of $\text{Ru}(\text{bpy})_3^{2+}$ by the catalytic reaction with TPrA-associated species (via eqs 4 and 5) and the positive feedback provided from the reduction of $\text{Ru}(\text{bpy})_3^{3+}$ on the substrate. The former is controlled by the diffusion of TPrA into the gap region, if the rates of the catalytic reactions are diffusion-limited, and thus has the same type of approach behavior as the irreversible oxidation of TPrA on the tip, which shows an approach curve characteristic of the tip over an insulating substrate.²¹

Figure 8B shows the tip current and ECL intensity approach curves over an insulating substrate, quartz. To increase the stability of the ECL intensity and tip current, the tip potential was pulsed (at 10-ms intervals) between 0.1 and 2.1 V with the tip current and ECL intensity sampled near the end of each pulse. Both the ECL intensity and tip current decreased

(18) Rubinstein, I.; Bard, A. J. *J. Am. Chem. Soc.* **1981**, *103*, 512.

(19) Leland, J. K.; Powell, M. J. *J. Electrochem. Soc.* **1990**, *137*, 3127.

(20) Nofsinger, J. B.; Danielson, N. D. *Anal. Chem.* **1987**, *59*, 865.

(21) Fan, F. - R.; Cliffel, D. E.; Bard, A. J., Manuscript in preparation.

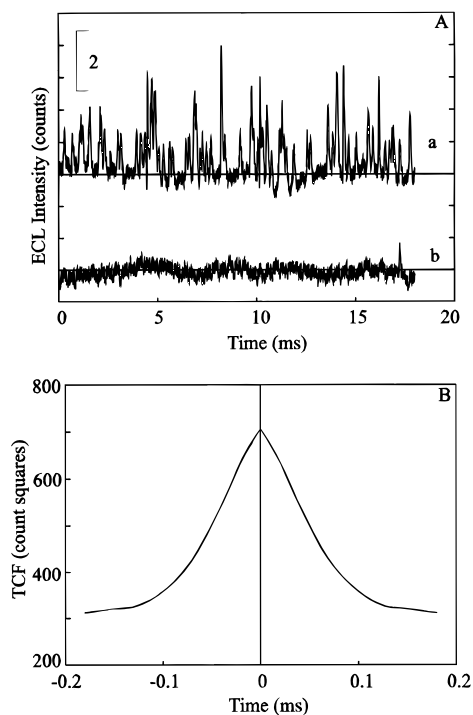


Figure 11. (A) Curve a: Histogram of the ECL intensity viewed at a sampling rate of 200 kHz. Tip far away from the ITO substrate. Conditions for ECL generation and the tip the same as those in Figure 9. Curve b: Background histogram. (B) Time correlation function (TCF) of curve a. ECL intensity experiments carried out with a Hamamatsu C1230 photon counter with a PMT R928P, which was cooled thermoelectrically to $-15\text{ }^{\circ}\text{C}$.

monotonically with decreasing distance and follow the theoretical SECM approach curve for an insulating substrate reasonably well. We conclude that the ECL intensity approach behavior is independent of the conducting nature of the substrate and follows the SECM tip current approach curve for an insulating substrate. This suggests that the rate constant of the excited-state generation reaction (eq 5) is close to the diffusion limit and the ECL intensity is controlled by the diffusion of TPrA and $\text{Ru}(\text{bpy})_3^{2+}$ into the gap region.

Stochastic Behavior and Statistical Analysis. Individual reaction events can be detected by recording the tip response with time during the oxidation of $\text{Ru}(\text{bpy})_3^{2+}$ and TPrA. Figure 9 shows three histograms of ECL intensity recorded for three different gap separations between the tip and ITO substrate;

the separations correspond to the two z positions marked A and B in Figure 8A (Figure 9A,B) and to a third position with the tip far away from the substrate (Figure 9C). The intensity spikes are quantized, as shown in Figure 10, where the probability density functions (PDF) show distributions of ECL intensity characteristic of discrete random events. The most probable ECL intensities are spaced ca. 0.1 V apart. Assuming that a photomultiplier tube output of 0.1 V represents the detection of a single photon, one can analyze the PDF and determine the mean rates of photon arrival. All three PDFs follow the Poisson density function (eq 3) (Figure 10D) and provide the relative mean photonic emission rate for the case of C:B:A = 16.1:1.1:1.1. With higher temporal resolution, the histogram of the ECL intensity for a tip far from the surface shows clearly the discrete nature of photon emission (Figure 11A). Its PDF is Poissonian and has a mean value of 0.51. Its time correlation function (TCF), as shown in Figure 11B, indicates that the coherence of the data is high and approximately follows the expected linear relation for a Poisson process in a short-time-scale range with a mean fluctuation rate of ca. $5 \times 10^4\text{ s}^{-1}$. Further studies are in progress to observe ECL events from single molecules.

Conclusions

Early studies have shown that single molecules can be trapped and detected electrochemically at electrodes and single reaction events of reactants generated at electrodes can be observed. These have involved soluble species and ultramicroelectrodes. It should also be possible to observe single molecules adsorbed on a surface, if a suitable amplification process, like ECL, can be developed. For example, we recently showed that DNA can be adsorbed on a suitably structured surface and detected by intercalation with $\text{Ru}(\text{phen})_3^{2+}$, which is oxidized in the presence of a coreactant (TPrA) to produce ECL emission.²² The process described did not show sufficient amplification to provide the needed sensitivity because the adsorbed DNA was removed during the ECL oxidation process. However, in principle, given sufficiently strong adsorption and reactant stability, single-molecule DNA detection would be possible.

AR9502442

(22) Xu, X-H.; Bard, A. J. *J. Am. Chem. Soc.* **1995**, *117*, 2627.